Mathematical Biosciences and Engineering

http://www.aimspress.com/journal/mbe

MBE, 19(8): 8452–8478.
DOI: 10.3934/mbe.2022393
Received: 11 April 2022
Revised: 18 May 2022
Accepted: 25 May 2022
Published: 09 June 2022

Research article

Modelling the dynamics of *Trypanosoma rangeli* and triatomine bug with logistic growth of vector and systemic transmission

Lin Chen[1], **Xiaotian Wu**[2], **Yancong Xu**[1,*] **and Libin Rong**[3]

[1] Department of Mathematics, Hangzhou Normal University, Hangzhou 311121, China
[2] College of Arts and Sciences, Shanghai Maritime University, Shanghai 201306, China
[3] Department of Mathematics, University of Florida, Gainesville 32611, USA

* **Correspondence:** Email: Yancongx@hznu.edu.cn.

Abstract: In this paper, an insect-parasite-host model with logistic growth of triatomine bugs is formulated to study the transmission between hosts and vectors of the Chagas disease by using dynamical system approach. We derive the basic reproduction numbers for triatomine bugs and *Trypanosoma rangeli* as two thresholds. The local and global stability of the vector-free equilibrium, parasite-free equilibrium and parasite-positive equilibrium is investigated through the derived two thresholds. Forward bifurcation, saddle-node bifurcation and Hopf bifurcation are proved analytically and illustrated numerically. We show that the model can lose the stability of the vector-free equilibrium and exhibit a supercritical Hopf bifurcation, indicating the occurrence of a stable limit cycle. We also find it unlikely to have backward bifurcation and Bogdanov-Takens bifurcation of the parasite-positive equilibrium. However, the sustained oscillations of infected vector population suggest that *Trypanosoma rangeli* will persist in all the populations, posing a significant challenge for the prevention and control of Chagas disease.

Keywords: chagas disease; *Trypanosoma rangeli*; logistic growth; pathogenic effect; Hopf bifurcation; forward bifurcation

1. Introduction

Chagas disease, known as American trypanosomiasis, is a protozoan parasitic disease caused by *Trypanosoma cruzi* (*T. cruzi*). The disease was discovered firstly by Doctor Chagas in 1908 and it was named after that. Chagas disease is an illness that can cause serious consequences including heart disease and cardiomyopathy, and many people infected with Chagas disease may die due to these complications [1, 2]. It is mainly prevalent in Central and South America, such as Argentina, Bolivia, Brazil, Chile, etc. About 13% of the Latin American population is at risk of *T. cruzi* infection

[3]. Due to convenient transportation and the globalization, Chagas disease is spreading very widely in the world, see Figure 1(a),(b) for details. An estimated 8 million people are infected with *Trypanosoma cruzi* worldwide, mainly in Latin America where Chagas disease remains one of the biggest public health problems, causing incapacity in infected individuals and more than 10,000 deaths per year [4–6]. In particular, patients with Chagas disease may be coinfected with other epidemic diseases including HIV [7] and COVID-19. These patients are at risk of severe COVID-19 manifestations and should be a priority group to be vaccinated [8].

Trypanosoma cruzi, a protozoan parasite that parasitizes human and mammalian blood and tissue cells, can be transmitted by blood-sucking triatomine bugs to cause the symptoms of Chagas disease. It is spread mainly through the faeces of the infected blood-sucking triatomine bugs. These bugs usually live in the crevices of poorly built houses in rural or suburban areas. They hide during the day and come out at night to feed on human blood. They bite exposed areas of the skin, such as the face, and defecate near the bites. If one scratches on the bites, this leads to feces spreading to the sites of eye, mouth, or any skin break, and then the parasites enter the body, and eventually go into the heart, survive and proliferate inside [3, 9]. Triatomine bugs, the vectors to transmit Chagas disease, have a relatively short life span, ranging from 4 to 14 months depending largely on species and environmental conditions. They suck the blood of vertebrates, especially mammals (such as dogs, bats, armadillos, squirrels, guinea pigs and humans), and then release feces on the skin of the bitten animal. The feeding time may take 10–30 minutes [10]. Once healthy triatomine bugs ingest with the parasites of Chagas disease, they will be infected quickly [11–13].

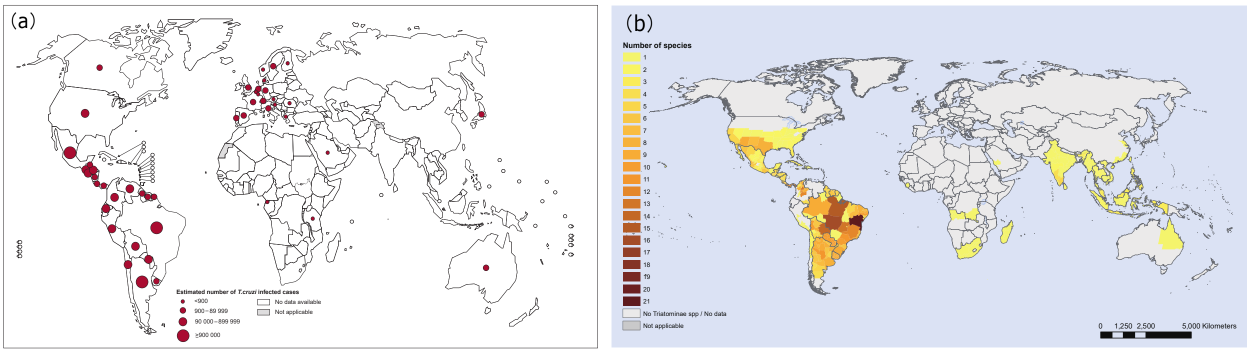

Figure 1. (a) Global distribution of cases of Chagas disease, based on the estimates in 2018. (b) Number of Triatominae species identified, at first administrative level in 2020. All data are from the World Healthy Organization (WHO) website, https://www.who.int/data/gho/data/countries.

Trypanosoma rangeli (*T. rangeli*) is a kind of parasite which is pathogenic to some vector species including triatomine bug, it always influence the transmission dynamics of the infected bugs, so this kind of transmission behavior deserves further research. *Rhodnius prolixus (R. prolixus)* is one of the triatomine species and *T. rangeli* is one of the trypanosoma which is spread between hosts and triatomine vectors. Although *T. rangeli* can infect mammals through the same triatomines, it is not pathogenic to human. However, it is still important to study the transmission dynamics of *T. rangeli* because it shares soluble antigenic epitopes with *T. cruzi* and the crossed serological reactions affect the diagnosis of Chagas disease [14, 15]. Both *T. rangeli* and *T. cruzi* have common hosts and triatomine vectors. The transmission dynamics of *T. rangeli* between hosts and triatomine bugs can affect the effectiveness of *T. cruzi* transmission [10]. Moreover, *T. rangeli* has pathogenic effect on triatomine bugs in the sense that the infection of *T. rangeli* can change the behavior of triatomine bugs, which alters the transmission of Chagas disease [14, 16]. There are some studies showing the possible interaction between *T. rangeli* and *T. cruzi* [17]. Therefore, it is essential to study the transmission behavior of *T. rangeli*. *T. rangeli*'s infection pattern is similar to that of *T. cruzi*. The healthy population will get infected if they bite the infected counterparts through systemic transmission, where *T. rangeli* parasite can enter and multiply at the common hosts' and vectors' bloodstream. In addition to this normal insect-host-insect transmission mode, there is another mode of *T. rangeli* transmission called insect-to-insect co-feeding transmission. Susceptible triatomine bugs can get infected if they are feeding with infected counterparts on the same hosts. This has been studied in some papers [10,18–22] and it differs from the transmission of *T. cruzi*.

There are a number of mathematical models that studied the transmission dynamics of Chagas disease, such as the different transmission routes of the interaction between hosts and vectors [2,23,24], the disease transmission in the host movement and host community composition [9, 16, 25–27], the triatomine population with temporal or spatial variations [28–33], and the optimal control of Chagas disease [34–38]. Recently, Wu et al. [10] formulated a new model by considering the Ricker's type growth of triatomine bugs and *T. rangeli*'s pathogenic effect on triatomine bugs. However, the logistic growth of triatomine bugs is very common but was not investigated in the model. In this paper, we assume the generation rate of triatomine bugs follows the logistic growth instead of Ricker's type function and further study the dynamical behavior of triatomine-rangeli-host transmission. The new model is shown to have interesting dynamics, provide more insights into the interaction between triatomine bugs and *T. rangeli*, and may help to prevent and control the Chagas disease.

The paper is outlined as follows. In the next section, we propose the model with logistic growth and T. rangli's pathogenic effect on triamine bugs. In Section 3, the existence and stability of vector-free equilibrium, parasite-free equilibrium and parasite-positive equilibrium are considered. In Section 4, the bifurcation analysis including forward bifurcation and Hopf bifurcation is studied. Numerical simulations are also performed in Section 5. Conclusion and discussion are given in Section 6.

2. Model

The model developed in the reference [10] is

$$\begin{aligned}
S_h'(t) &= \Lambda_h - \tilde{\beta}_h I_v(t) S_h(t) - \mu_1 S_h(t),\\
I_h'(t) &= \tilde{\beta}_h I_v(t) S_h(t) - \mu_1 I_h(t),\\
S_v'(t) &= r(S_v(t) + \theta I_v(t)) e^{-\sigma(S_v(t)+I_v(t))} - \tilde{\beta}_v S_v(t) I_h(t) - \beta_c S_v(t) I_v(t) - \mu_2 S_v(t),\\
I_v'(t) &= \tilde{\beta}_v S_v(t) I_h(t) + \beta_c S_v(t) I_v(t) - d I_v(t) - \mu_2 I_v(t),
\end{aligned} \tag{2.1}$$

where the population is divided into four compartments: susceptible and infected competent hosts, susceptible and infected triatomine bugs, denoted by S_h, I_h, S_v, I_v in order. Λ_h is the constant recruitment rate of susceptible competent host per unit time. The transmission rate from infected bugs to susceptible competent hosts is denoted by $\tilde{\beta}_h = \frac{ba}{N_c+\alpha N_q}$, where b is the transmission probability from infected bugs to susceptible competent hosts per bite, a is the number of bites per triatomine bug per unit time, α is the biting preference of quasi-competent hosts to competent hosts, N_c is the total number of competent hosts, and N_q is the total number of quasi-competent hosts. The transmission rate from infected competent hosts to susceptible bugs is denoted by $\tilde{\beta}_v = \frac{ca}{N_c+\alpha N_q}$, where c is the transmission probability from infected hosts to susceptible triatomine bug per bite. The total infection rate through co-feeding transmission between susceptible and infected bugs is β_c, which is transmitted by both the competent and quasi-competent hosts. Here $\beta_c = \frac{1}{\delta}\beta_{ch}N_c(\frac{a}{N_c+\alpha N_q}\frac{\tau_1}{\omega})^2 + \frac{1}{\delta}\beta_{cq}N_q(\frac{a\alpha}{N_c+\alpha N_q}\frac{\tau_2}{\omega})^2$, where ω is the unit time, δ is the ratio of night to unit time, β_{ch} and β_{cq} are the transmission rates from infected bugs to susceptible bugs on an average competent host and quasi-competent host during night, respectively. τ_1 and τ_2 are the feeding times per bite on a competent host and a quasi-competent host, respectively. The Ricker's type function $b(x) = rxe^{-\sigma x}$ was chosen to model the reproduction rate of R. prolixus. Integrating the pathogenic effect, the growth rate of triatomine bugs is modeled as $r(S_v + \theta I_v)e^{-\sigma(S_v+I_v)}$, where r is the maximal number of offsprings that a triatomine bug can produce per unit time, $\theta \in [0, 1]$ is the reproduction reduction of bugs due to the pathogenic effect of *T. rangeli* on bugs, σ is the density-dependency strength measuring the reproduction of bugs. μ_1 and μ_2 are the natural death rates of competent hosts and triatomine bugs, respectively. d is the death rate of infected vectors induced by pathogenic effect.

Model (2.1) includes the systemic and co-feeding transmission routes among vectors and hosts. Two thresholds were derived to study the dynamical behavior of this model [10]. Sustained oscillations were found numerically by changing the parameters d and θ. Furthermore, the oscillation amplitude is larger if d is larger or θ is smaller.

In this paper, we assume the generation rate of triatomine bugs follows the logistic growth instead of Ricker's type function. Here we only consider the systemic transmission, then model (2.1) can be changed to

$$\begin{aligned}
S_h'(t) &= \Lambda_h - \beta_h I_v(t)S_h(t) - \mu_1 S_h(t),\\
I_h'(t) &= \beta_h I_v(t)S_h(t) - \mu_1 I_h(t),\\
S_v'(t) &= r(S_v(t) + \theta I_v(t))(1 - \frac{S_v(t)+I_v(t)}{K}) - \beta_v S_v(t)I_h(t) - \mu_2 S_v(t),\\
I_v'(t) &= \beta_v S_v(t)I_h(t) - dI_v(t) - \mu_2 I_v(t),
\end{aligned} \tag{2.2}$$

where $\beta_h = \frac{ba}{N_h}, \beta_v = \frac{ca}{N_h}$, N_h is the total number of hosts. The infection rate of susceptible competent hosts after bugs' biting at time t is $\beta_h I_v(t)S_h(t)$, and the infection rate of susceptible vectors after bugs' biting at time t is $\beta_v S_v(t)I_h(t)$. In the logistic growth $r(S_v + \theta I_v)(1 - \frac{S_v+I_v}{K})$ of triatomine bugs, K is the carrying capacity. The other parameters are the same as those in model (2.1). All the parameters are non-negative and their biological meanings and ranges are given in Table 1.

Denote the total population of competent hosts by $N_h = S_h + I_h$. Adding the first and second equations leads to

$$N_h'(t) = \Lambda_h - \mu_1 N_h(t).$$

It follows that

$$\lim_{t\to\infty} N_h(t) = \frac{\Lambda_h}{\mu_1} \triangleq N_h.$$

Thus, in the limiting system we have $S_h(t) = N_h - I_h(t)$.

Table 1. Parameters of model (2.2).

Parameter	Range	Description
Λ_h	varied	Recruitment rate of susceptible competent host per unit time [10,39]
a	[0.2, 33]/day	Number of bites per triatomine bug per unit time [10,39]
b	[0.00271, 0.06]	Transmission probability from infected bugs to susceptible competent hosts per bite [2,9,10]
c	[0.00026, 0.49]	Transmission probability from infected hosts to susceptible triatomine bug per bite [9,25]
r	[0.0274, 0.7714]/day	Maximum number of offsprings that a triatomine bug can produce per unit time [2,25]
θ	[0, 1]	Reproduction reduction of bugs due to the infection of parasites [10]
N_h	varied	Total number of hosts [2]
K	varied	Carrying capacity [10]
μ_1	[0.000038, 0.0025]/day	Natural death rate of hosts [9,25]
μ_2	[0.0045, 0.0083]/day	Natural death rate of triatomine bugs [9,25]
d	[0.0188, 0.0347]/day	Death rate of infected vectors due to pathogenic effect [10]

Accordingly, system (2.2) can be reduced to the following three-dimensional limiting system:

$$\begin{aligned} I_h'(t) &= \beta_h I_v(t)(N_h - I_h(t)) - \mu_1 I_h(t), \\ S_v'(t) &= r(S_v(t) + \theta I_v(t))(1 - \frac{S_v(t) + I_v(t)}{K}) - \beta_v S_v(t) I_h(t) - \mu_2 S_v(t), \\ I_v'(t) &= \beta_v S_v(t) I_h(t) - d I_v(t) - \mu_2 I_v(t). \end{aligned} \tag{2.3}$$

It is easy to know that the feasible region of system (2.3) is

$$D = \{(I_h, S_v, I_v) | 0 \le I_h \le N_h, 0 \le S_v, 0 \le I_v, S_v + I_v \le K\}.$$

3. Existence and stability of equilibria

3.1. Existence of equilibria

Let the right-hand side of the equations of system (2.3) be zero. There are one vector-free equilibrium $E_0(0,0,0)$ and one parasite-free equilibrium $E_S(0, \frac{K(r-\mu_2)}{r}, 0)$. We will derive two thresholds R_v and R_0 to study the dynamic behavior of system (2.3) where R_v is the triatomine bug basic reproduction number and R_0 is the *T. rangeli* basic reproduction number.

The Jacobian matrix of system (2.3) at the vector-free equilibrium $E_0(0,0,0)$ is

$$J(E_0) = \begin{pmatrix} -\mu_1 & 0 & \beta_h N_h \\ 0 & r - \mu_2 & \theta r \\ 0 & 0 & -(d + \mu_2) \end{pmatrix}.$$

The eigenvalues of the Jacobian matrix $J(E_0)$ at $E_0(0,0,0)$ are $-\mu_1, -(d+\mu_2)$ and $r - \mu_2$, respectively. Let

$$R_v = \frac{r}{\mu_2}.$$

We will show that it provides a threshold to determine the persistence or extinction of the vector population.

For the parasite-free equilibrium $E_S(0, S_v^0, 0)$ with $S_v^0 = \frac{K(r-\mu_2)}{r}$ to be biologically feasible, we need $r - \mu_2 > 0$, namely, $R_v > 1$. Next, we calculate the *T. rangeli* basic reproduction number R_0 of system (2.3). Using the method in ref. [40], we have

$$F = \begin{pmatrix} 0 & 0 & N_h\beta_h \\ 0 & 0 & 0 \\ \frac{K(r-\mu_2)}{r}\beta_v & 0 & 0 \end{pmatrix},$$

$$V = \begin{pmatrix} \mu_1 & 0 & 0 \\ \frac{K(r-\mu_2)}{r}\beta_v & r-\mu_2 & r - r\theta(1-\frac{r-\mu_2}{r}) - \mu_2 \\ 0 & 0 & d+\mu_2 \end{pmatrix}.$$

Thus, the *T. rangeli* basic reproduction number of system (2.3), given by the spectral radius of the next generation matrix, is

$$R_0 = \rho(FV^{-1}) = \sqrt{\frac{a^2bcK(r-\mu_2)}{rN_h\mu_1(d+\mu_2)}} = \sqrt{\frac{\beta_h\beta_v N_h S_v^0}{(d+\mu_2)\mu_1}}, \tag{3.1}$$

where $S_v^0 = \frac{K(r-\mu_2)}{r}$.

For any parasite-positive equilibrium $E^* = (I_h^*, S_v^*, I_v^*)$ of system (2.3), its elements satisfy

$$S_v^* = \frac{\mu_1(d+\mu_2)}{\beta_h\beta_v(N_h - I_h^*)},\ I_v^* = \frac{\mu_1 I_h^*}{\beta_h(N_h - I_h^*)}, \tag{3.2}$$

and I_h^* is the positive root of the following equation:

$$f(I_h^*) = A(I_h^*)^2 + BI_h^* + C = 0, \tag{3.3}$$

where

$$\begin{aligned} A &= \tfrac{a^2c^2\mu_1}{N_h}(abK(r\theta - d - \mu_2) + \theta r N_h\mu_1), \\ B &= ac\mu_1(abK(ac(d+\mu_2-r\theta) + (r-\mu_2)(d+\mu_2)) + rN_h\mu_1(d+\mu_2)(\theta+1)), \\ C &= N_h\mu_1(a^2bcK(\mu_2 - r)(d+\mu_2) + rN_h\mu_1(d+\mu_2)^2) = (N_h\mu_1)^2(d+\mu_2)^2(1-R_0^2). \end{aligned}$$

Let $\Delta = B^2 - 4AC$. We have

$$\begin{aligned} \Delta =& a^2c^2\mu_1^2[-4(d+\mu_2)(rN_h\mu_1(d+\mu_2) + a^2bcK(\mu_2 - r))(\theta r N_h\mu_1 - abK(d+\mu_2-r\theta)) \\ &+ (rN_h\mu_1(\theta+1)(d+\mu_2) + abK((d+\mu_2)(r-\mu_2) + ac(d+\mu_2-r\theta)))^2]. \end{aligned}$$

If $\Delta \geq 0$, then the equation $f(I_h^*) = 0$ may have two roots, which are denoted by

$$I_{h1}^* = \frac{-B-\sqrt{\Delta}}{2A},\ I_{h2}^* = \frac{-B+\sqrt{\Delta}}{2A}.$$

From (3.2), we can see that $S_v^* > 0, I_v^* > 0$ as long as $I_h^* > 0$. Therefore, we study the existence of the parasite-positive equilibria in the following cases:

1) $R_0 = 1$, namely, $a^2bcK(r-\mu_2) = rN_h\mu_1(d+\mu_2)$.
In this case, we have $B > 0, C = 0, \Delta > 0, A = \frac{ac\mu_1^2}{r-\mu_2}((d+\mu_2)(r\theta-d-\mu_2)+acr\theta(r-\mu_2))$. By Vieta theorem, if $A > 0$, then $I_{h1}^* < 0, I_{h2}^* = 0$. Thus, system (2.3) has no parasite-positive equilibrium. If $A < 0$, then $I_{h1}^* = 0, I_{h2}^* > 0$, and system (2.3) has a unique parasite-positive equilibrium $E_2(I_{h2}^*, S_v^*(I_{h2}^*), I_v^*(I_{h2}^*))$. If $A = 0$, then Eq (3.3) has a zero root, i.e., there is no parasite-positive equilibrium of system (2.3).

2) $R_0 > 1$, namely, $a^2bcK(r-\mu_2) > rN_h\mu_1(d+\mu_2)$.
In this case, we have $B > 0, C < 0$. If $A > 0$, then $\Delta > 0$, $I_{h1}^* < 0, I_{h2}^* > 0$, and system (2.3) has a unique parasite-positive equilibrium $E_2(I_{h2}^*, S_v^*(I_{h2}^*), I_v^*(I_{h2}^*))$. If $A < 0, \Delta > 0$, then $I_{h1}^* > 0, I_{h2}^* > 0$, and system (2.3) has two parasite-positive equilibria $E_1(I_{h1}^*, S_v^*(I_{h1}^*), I_v^*(I_{h1}^*))$ and $E_2(I_{h2}^*, S_v^*(I_{h2}^*), I_v^*(I_{h2}^*))$. If $A < 0, \Delta = 0$, then $E_1 = E_2$, which means that there is a parasite-positive equilibrium of multiplicity 2. If $A < 0, \Delta < 0$, then there is no parasite-positive equilibrium. If $A = 0$, there exists only one root of Eq (3.3) and the root is positive, i.e., one parasite-positive equilibrium $E^*(I_h^*, S_v^*(I_h^*), I_v^*(I_h^*))$ of system (2.3).

3) $R_0 < 1$, namely, $a^2bcK(r-\mu_2) < rN_h\mu_1(d+\mu_2)$.
In this case, we have $B > 0, C > 0$. If $A < 0$, then $\Delta > 0$, $I_{h1}^* < 0, I_{h2}^* > 0$, and system (2.3) has a unique parasite-positive equilibrium $E_2(I_{h2}^*, S_v^*(I_{h2}^*), I_v^*(I_{h2}^*))$. If $A \geq 0$, there is no positive root of (3.3), i.e., there is no parasite-positive equilibrium of system (2.3).

We summarize the results as follows:

Theorem 3.1 For system (2.3), we have the following results on the existence of equilibria.

1) The vector-free equilibrium $E_0(0,0,0)$ always exists. The parasite-free equilibrium $E_S(0, \frac{K(r-\mu_2)}{r}, 0)$ exists if and only if $R_v > 1$.
2) When $R_0 \leq 1$, there is a unique parasite-positive equilibrium E_2 if $A < 0$; Otherwise, there is no parasite-parasite-positive equilibrium.
3) When $R_0 > 1$, there is a unique parasite-positive equilibrium if $A \geq 0$, and there are two parasite-positive equilibria E_1 and E_2 if $A < 0, \Delta > 0$, and the two equilibria coalesce to E if and only if $A < 0, \Delta = 0$.

3.2. Stability of equilibria

3.2.1. Stability of vector-free and parasite-free equilibria

Theorem 3.2 The vector-free equilibrium $E_0(0,0,0)$ of system (2.3) is globally asymptotically stable if $R_v < 1$ and unstable if $R_v > 1$.

Proof. At the vector-free equilibrium $E_0(0,0,0)$, the eigenvalues of the Jacobian matrix of system (2.3) are $-\mu_2, -(d+\mu_2)$ and $r-\mu_2$. If $R_v = \frac{r}{\mu_2} > 1$, namely, $r > \mu_2$, then there are two negative eigenvalues and one positive eigenvalue, i.e., E_0 is unstable. If $R_v < 1$, then all the eigenvalues are real and negative, which indicates that E_0 is locally asymptotically stable for $R_v < 1$.

Let $N_v = S_v + I_v$. We have

$$
\begin{aligned}
N_v' &= S_v' + I_v' \\
&= r(S_v(t) + \theta I_v(t))\left(1 - \frac{S_v(t) + I_v(t)}{K}\right) - \mu_2 S_v(t) - dI_v - \mu_2 I_v \\
&\leq rN_v(1 - \frac{N_v}{K}) - \mu_2 N_v \\
&\leq (r - \mu_2)N_v.
\end{aligned}
$$

Thus, we have

$$
\limsup_{t\to\infty} N_v(t) \leq \lim_{t\to\infty} N_v(0)e^{(r-\mu_2)t} = 0,
$$

with any feasible initial solution $N_v(0) = S_v(0) + I_v(0)$ when $R_v < 1$. That is to say, the solutions of S_v and I_v with any feasible initial conditions will tend to zeroes if $R_v < 1$. For subsystem of I_h, it is cooperative with the positive invariance set $[0, N_h]$. The vector-free equilibrium E_0 is unique for system (2.3) if $R_v < 1$. From this, we know that E_0 is globally asymptotically stable if $R_v < 1$.

Theorem 3.3 The parasite-free equilibrium $E_S(0, \frac{K(r-\mu_2)}{r}, 0)$ of system (2.3) is
1) a saddle-node point when $R_0 = 1$;
2) unstable when $R_0 > 1$;
3) locally asymptotically stable when $R_0 < 1$.

Proof. At the parasite-free equilibrium $E_S(0, S_v^0, 0)$, where $S_v^0 = \frac{K(r-\mu_2)}{r}$, the Jacobian matrix of system (2.3) is

$$
J(E_S) = \begin{pmatrix} -\mu_1 & 0 & N_h\beta_h \\ -S_v^0\beta_v & \mu_2 - r & (1+\theta)\mu_2 - r \\ S_v^0\beta_v & 0 & -d-\mu_2 \end{pmatrix}. \tag{3.4}
$$

The corresponding characteristic polynomial of (3.4) is

$$
P(\lambda) = -(\lambda + r - \mu_2)[\lambda^2 + b_0\lambda + c_0], \tag{3.5}
$$

where

$$
b_0 = \mu_1 + \mu_2 + d,\ c_0 = \mu_1(d + \mu_2) - \frac{a^2bcK(r-\mu_2)}{rN_h}.
$$

The eigenvalues of system (2.3) at E_S are the roots of $P(\lambda) = 0$ and denoted by λ_1, λ_2, and λ_3.
Let $\Delta_0 = b_0^2 - 4c_0$, i.e.,

$$
\Delta_0 = \frac{4a^2bcK(r-\mu_2)}{rN_h} + (d - \mu_1 + \mu_2)^2.
$$

Then the eigenvalues of (3.5) are

$$
\lambda_1 = \mu_2 - r, \lambda_2 = \frac{-b_0 - \sqrt{\Delta_0}}{2}, \lambda_3 = \frac{-b_0 + \sqrt{\Delta_0}}{2}.
$$

Since $r > \mu_2$, we have $\Delta_0 > 0$, which means that λ_2, λ_3 are real.
When $R_0 = 1$, we have $c_0 = 0, b_0 = \sqrt{\Delta_0}$. Therefore, $\lambda_1 = \mu_2 - r < 0, \lambda_2 = -b_0 = -d - \mu_1 - \mu_2 < 0$ and

$\lambda_3 = 0$. Because of the zero eigenvalue, we need to further study the type of E_S.

We let $x = I_h, y = S_v - S_v^0, z = I_v$ and shift the equilibrium to the origin. System (2.3) becomes

$$\begin{aligned}
x' &= abz + x(-\frac{abz}{N_h} - \mu_1),\\
y' &= -rz - \frac{ry^2}{K} - \frac{acKx}{N_h} - \frac{r\theta z^2}{K} + \mu_2 z + \frac{acK\mu_2 x}{rN_h} + \theta\mu_2 z + y(-r - \frac{acx}{N_h} - \frac{rz}{K} - \frac{r\theta z}{K} + \mu_2),\\
z' &= \frac{acxy}{N_h} + \frac{acKx}{N_h} + z(-d - \mu_2) - \frac{acK\mu_2 x}{rN_h}.
\end{aligned} \tag{3.6}$$

Then we make the following transformations

$$x = m_1 X + m_2 Z, y = m_3 X + Y + m_4 Z, z = X + Z,$$

where

$$m_1 = \frac{ab}{\mu_1}, m_2 = -\frac{ab}{d + \mu_2}, m_3 = -\frac{d + r - \theta\mu_2}{r - \mu_2}, m_4 = -\frac{(1+\theta)\mu_2 + \mu_1 - r}{d - r + \mu_1 + 2\mu_2}.$$

This leads to the following system

$$\begin{aligned}
X' &= -\frac{ab((r-\mu_2)(d+\mu_2) + ac(d + r - \theta\mu_2))}{N_h(r-\mu_2)(d+\mu_1+\mu_2)} X^2 + XO(|Y,Z|) + O(|Y,Z|^2),\\
Y' &= (\mu_2 - r)Y + O(|X,Y,Z|^2),\\
Z' &= (-d - \mu_1 - \mu_2)Z + O(|X,Y,Z|^2).
\end{aligned} \tag{3.7}$$

We know that E_S is a saddle-node point when $R_0 = 1$. Moreover, if $R_0 > 1$, then $\lambda_1 < 0, \lambda_2 < 0, \lambda_3 > 0$, i.e., E_S is unstable; if $R_0 < 1$, then $\lambda_1 < 0, \lambda_2 < 0, \lambda_3 < 0$, i.e., E_S is locally asymptotically stable.

Based on the above analysis, we conclude that the parasite-free equilibrium E_S of system (2.3) is a saddle-node point when $R_0 = 1$, unstable when $R_0 > 1$, and locally asymptotically stable when $R_0 < 1$ [41].

3.2.2. Stability of the unique parasite-positive equilibrium

In this section, we will study the global stability of the unique parasite-positive equilibrium E_1 by Li-Muldowney global-stability criterion [42] when $R_0 > 1$, $R_v > 1$ and $A \geq 0$.

Let $|\cdot|$ denote a vector norm in R^n and the induced matrix norm in $R^{n\times n}$, the space of all $n \times n$ matrices. For matrix A in $R^{n\times n}$, the Lozinskĩ measure or the logarithmic norm of A with respect to $|\cdot|$ [43] is

$$\mu(A) = \lim_{h\to 0^+} \frac{|I + hA| - 1}{h}.$$

Let $y(t)$ be a solution of linear differential equation

$$y'(t) = A(t)y(t),$$

where $A(t)$ is $m \times m$ matrix-valued continuous function. For $t \geq t_0$, we have

$$|y(t)| \leq |y(t_0)| e^{\int_{t_0}^{t} \mu(A(t))dt}.$$

Let B be an $n \times n$ matrix. The second additive compound matrix of B, denoted by $B^{[2]}$, is an $\binom{n}{2} \times \binom{n}{2}$ matrix. For instance, if $B = (b_{ij})$ is a 3×3 matrix, then

$$B^{[2]} = \begin{pmatrix} b_{11} + b_{22} & b_{23} & -b_{13} \\ b_{32} & b_{11} + b_{33} & b_{12} \\ -b_{31} & b_{21} & b_{22} + b_{33} \end{pmatrix}.$$

Consider the following autonomous system

$$x' = f(x), \tag{3.8}$$

where $f : \Omega \to R^n, \Omega \subset R^n$ is an open set, simply connected, and $f \in C^1(\Omega)$. Let $x(t, x_0)$ be the solution of system (3.8) such that $x(0, x_0) = x_0$. Suppose x^* is an equilibrium of system (3.8), i.e., $f(x^*) = 0$. A set K is said to be absorbing in Ω for system (3.8) if $x(t, K_1) \subset K$ for each compact set $K_1 \subset \Omega$ and sufficiently large t. Assume the following assumptions hold:
(H_1) System (3.8) has a unique equilibrium point x^* in Ω.
(H_2) System (3.8) has a compact absorbing set $K \subset \Omega$.
Let $Q : \Omega \mapsto Q(x)$ be $\binom{n}{2} \times \binom{n}{2}$ matrix-valued function with its inverse $Q^{-1}(x)$. Let μ be a Lozinskĩ measure on $R^{N\times N}$, where $N = \binom{n}{2}$. Define

$$\bar{q}_2 = \lim_{t\to\infty} \sup \sup_{x_0 \in K} \frac{1}{t} \int_0^1 \mu(X(x(s, x_0)))ds,$$

where

$$X = Q_f Q^{-1} + QJ^{[2]} Q^{-1},$$

the matrix Q_f is obtained by replacing each entry q_{ij} of Q by its derivative in the direction of f, $(q_{ij})f$, and $J^{[2]}$ is the second additive compound matrix of the Jacobian matrix J of system (3.8).
Lemma 3.1 [42] Assume that Ω is simply connected and assumptions (H_1) and (H_2) hold. Then, the unique equilibrium x^* of system (3.8) is globally asymptotically stable in Ω if there exist a function Q and a Lozinskĩ measure μ such that $\bar{q}_2 < 0$.

We have the following theorem for our model.
Theorem 3.4 Assume that $R_0 > 1$, $R_v > 1$ and $A \geq 0$. The unique parasite-positive equilibrium E_1 of system (2.3) is globally asymptotically stable if $\sigma = K^2\beta_v + \tilde{v} < 0$, where

$$\begin{aligned} \tilde{v} &= \max\{v_1, v_2\}, \\ v_1 &= -\tfrac{r(S_v^2 + I_v(K-I_v)\theta) + S_v K(I_v\beta_h + \mu_1)}{S_v K} + \max\{|\tfrac{I_v r(S_v + (2I_v + S_v - K)\theta)}{S_v K}|, \tfrac{I_v(N_h - I_h)\beta_h}{S_v}\}, \\ v_2 &= \max\{-I_v\beta_h - S_v\beta_v - \mu_1, \tfrac{r(K-2S_v) - I_v r(1+\theta) - K(I_h\beta_v + \mu_2)}{K}\}. \end{aligned} \tag{3.9}$$

Proof. When $R_0 > 1$, $R_v > 1$ and $A \geq 0$, it is easy to show the uniqueness of the parasite-positive equilibrium E_1. By Theorems 3.2 and 3.3, we know that the vector-free equilibrium E_0 and the parasite-free equilibrium E_S are unstable when $R_v > 1$ and $R_0 > 1$. It can also be checked that the conditions (H_1) and (H_2) are satisfied. Next we show the global stability of the unique parasite-positive equilibrium $E_1(I_h, S_v, I_v)$.

The Jacobian matrix of system (2.3) at E_1 is

$$J = \begin{pmatrix} -I_v\beta_h - \mu_1 & 0 & (N_h - I_h)\beta_h \\ -S_v\beta_v & J_{22} & J_{23} \\ S_v\beta_v & I_h\beta_v & -d - \mu_2 \end{pmatrix},$$

where $J_{22} = r(1-\frac{I_v+S_v}{K})-I_h\beta_v-\mu_2-\frac{r(S_v+\theta I_v)}{K}$, $J_{23} = r\theta(1-\frac{I_v+S_v}{K})-\frac{r(S_v+\theta I_v)}{K}$. The second additive compound matrix $J^{[2]}$ is

$$J^{[2]} = \begin{pmatrix} -I_v\beta_h-\mu_1+J_{22} & J_{23} & -(N_h-I_h)\beta_h \\ I_h\beta_v & -I_v\beta_h-\mu_1-d-\mu_2 & 0 \\ -S_v\beta_v & -S_v\beta_v & J_{22}-d-\mu_2 \end{pmatrix}.$$

Let $P(I_h,S_v,I_v) = \text{diag}(1,\frac{S_v}{I_v},\frac{S_v}{I_v})$. Then $P_f = \text{diag}(0,\frac{\dot{S_v}}{I_v}-\frac{S_v\dot{I_v}}{I_v^2},\frac{\dot{S_v}}{I_v}-\frac{S_v\dot{I_v}}{I_v^2})$. We have $P_fP^{-1} = \text{diag}(0,\frac{S_v'}{S_v}-\frac{I_v'}{I_v},\frac{S_v'}{S_v}-\frac{I_v'}{I_v})$, and let $B = P_fP^{-1}+PJ^{[2]}P^{-1}$.
From system (2.3), we obtain

$$\begin{aligned} \frac{S_v'}{S_v} &= r-\mu_2-\frac{S_v(rS_v+I_hK\beta_v)+I_v^2r\theta+I_vr(S_v+S_v\theta-K\theta)}{S_vK}, \\ \frac{I_v'}{I_v} &= -d-\mu_2+\frac{I_hS_v\beta_v}{I_v}. \end{aligned}$$

Straightforward calculations yield

$$B = \begin{pmatrix} B_{11} & B_{12} \\ B_{21} & B_{22} \end{pmatrix},$$

where

$$\begin{aligned} B_{11} &= \frac{r(K-2S_v)-I_v(r+r\theta+K\beta_h)-K(I_h\beta_v+\mu_1+\mu_2)}{K}, \\ B_{12} &= (-\frac{I_vr(S_v+(2I_v+S_v-K)\theta)}{S_vK},\frac{I_v(I_h-N_h)\beta_h}{S_v}), \\ B_{21} &= (\frac{I_hS_v\beta_v}{I_v},-\frac{S_v^2\beta_v}{I_v})^T, \end{aligned}$$

$$B_{22} = \begin{pmatrix} -d-I_v\beta_h-\mu_1-\mu_2-\frac{I_v'}{I_v}+\frac{S_v'}{S_v} & 0 \\ -S_v\beta_v & \frac{r(K-2S_v)-I_vr(1+\theta)-K(d+I_h\beta_v+2\mu_2)}{K}-\frac{I_v'}{I_v}+\frac{S_v'}{S_v} \end{pmatrix}.$$

Take the norm $|(I_h,S_v,I_v)| = \max\{|I_h|,|S_v|+|I_v|\}$ in R^3. $\mu(\cdot)$ is the Lozinskĩ measure with the vector norm [44]. We have

$$\mu_B \le \sup\{g_1,g_2\} = \sup\{\mu_1(B_{11})+|B_{12}|,\mu_1(B_{22})+|B_{21}|\},$$

where $|B_{12}|,|B_{21}|$ are the matrix norms with respect to l_1 vector norm.
Calculations show that

$$\begin{aligned} \mu_1(B_{11}) &= \frac{r(K-2S_v)-I_v(r+r\theta+K\beta_h)-K(I_h\beta_v+\mu_1+\mu_2)}{K}, \\ |B_{12}| &= \max\{|\frac{I_vr(S_v+(2I_v+S_v-K)\theta)}{S_vK}|,\frac{I_v(N_h-I_h)\beta_h}{S_v}\}, \\ |B_{21}| &= \frac{I_hS_v\beta_v}{I_v}+\frac{S_v^2\beta_v}{I_v}, \\ \mu_1(B_{22}) &= -\frac{I_v'}{I_v}+\frac{S_v'}{S_v}-d-\mu_2+v_2. \end{aligned}$$

Thus, we have

$$g_1 = \frac{S_v^{'}}{S_v} + v_1 \le \frac{S_v^{'}}{S_v} + \tilde{v},$$
$$g_2 = \frac{S_v^2\beta_v}{I_v} + \frac{S_v^{'}}{S_v} + v_2 \le \frac{S_v^{'}}{S_v} + \frac{S_v^2\beta_v}{I_v} + \tilde{v},$$
$$\mu_B \le \frac{S_v^{'}}{S_v} + \frac{S_v^2\beta_v}{I_v} + \tilde{v},$$

where $\tilde{v}$, v_1, v_2 are defined by (3.9).

According to $S_v + I_v \le K$, we have $\mu_B \le \frac{S_v^{'}}{S_v} + K^2\beta_v + \tilde{v}$, that is

$$\mu_B \le \frac{S_v^{'}}{S_v} + \sigma,$$

where $\sigma = K^2\beta_v + \tilde{v}$.

Along each solution $(I_h, S_v, I_v) \subset D$ of system (2.3), then for $t > \bar{t}$, we have

$$\begin{aligned} \frac{1}{t}\int_0^t \mu(B)ds &= \frac{1}{t}\int_0^{\bar{t}} \mu(B)ds + \frac{1}{t}\int_{\bar{t}}^t \mu(B)ds \\ &\le \frac{1}{t}\int_0^{\bar{t}} \mu(B)ds + \frac{1}{t}\ln\frac{S_v(t)}{S_v(\bar{t})} + \frac{t-\bar{t}}{t}\sigma, \end{aligned}$$

which means that $\bar{q_2} \le \sigma < 0$. This completes the proof.

T. rangeli may not be pathogenic to every triatomine species [17]. Thus, we also study the dynamics of system (2.3) in the absence of pathogenic effect on triatomine bugs, i.e., $d = 0$ and $\theta = 1$. This allows us to compare the obtained results with and without the pathogenic effect.

Theorem 3.5 Assume $R_v > 1$ and $R_0 > 1$. In the absence of pathogenic effect on triatomine bugs, namely, $\theta = 1$ and $d = 0$, system (2.3) admits a unique parasite-positive equilibrium $E^* = (I_h^*, S_v^*, I_v^*)$, which is locally asymptotically stable when $d^* > 0$, unstable when $d^* < 0$, where d^* is defined by (3.13).

Proof. In the case of $\theta = 1, d = 0$, system (2.3) becomes

$$\begin{aligned} I_h'(t) &= \beta_h I_v(t)(N_h - I_h(t)) - \mu_1 I_h(t), \\ S_v'(t) &= r(S_v(t) + I_v(t))(1 - \frac{S_v(t) + I_v(t)}{K}) - \beta_v S_v(t) I_h(t) - \mu_2 S_v(t), \\ I_v'(t) &= \beta_v S_v(t) I_h(t) - \mu_2 I_v(t). \end{aligned} \tag{3.10}$$

According to Theorem 3.1, the system (3.10) has a unique parasite-positive equilibrium $E^* = (I_h^*, S_v^*, I_v^*)$ when $R_0 > 1$. Adding the second and third equations of system (3.10), we have

$$N_v' = rN_v(1 - \frac{N_v}{K}) - \mu_2 N_v. \tag{3.11}$$

Letting the right-hand side of equation (3.11) be equal to zero, we obtain a unique parasite-positive equilibrium $N_v^* = S_v^0$ if $R_v > 1$, and a unique zero equilibrium which is globally asymptotically stable if $R_v \leq 1$.

When $R_v > 1$, the limiting system of system (3.10) can be reduced to

$$\begin{aligned} I_h'(t) &= \beta_h I_v(t)(N_h - I_h(t)) - \mu_1 I_h(t), \\ I_v'(t) &= \beta_v I_h(t)(S_v^0 - I_v) - \mu_2 I_v(t). \end{aligned} \tag{3.12}$$

System (3.12) has an unstable parasite-free equilibrium $(0,0)$. When $R_0 > 1$, there is a unique parasite-positive equilibrium $E_1 = (I_h^*, I_v^*)$, where S_v^* is replaced by $S_v^0 - I_v^*$ for susceptible vectors at equilibrium. The Jacobian matrix of system (3.12) at E_1 is

$$J(E_1) = \begin{pmatrix} -\beta_h I_v^* - \mu_1 & \beta_h(N_h - I_h^*) \\ \beta_v(S_v^0 - I_v^*) & -\beta_v I_h^* - \mu_2 \end{pmatrix}.$$

It is easy to know that the trace of $J(E_1)$ is negative. The determinant of $J(E_1)$ is

$$\det(J(E_1)) = \beta_h\beta_v N_h I_v^* - \beta_h\beta_v S_v^0(N_h - I_h^*) + \beta_v\mu_1 I_h^* + \beta_h\mu_2 I_v^* + \mu_1\mu_2 \triangleq d^*. \tag{3.13}$$

The eigenvalues of Jacobian matrix $J(E_1)$ have negative real parts when $d^* > 0$. When $d^* < 0$, one of the eigenvalues of Jacobian matrix $J(E_1)$ has a negative real part and the other has a positive real part. Therefore, the equilibrium $E_1(I_h^*, I_v^*)$ of system (2.3) is locally asymptotically stable if $d^* > 0$, unstable if $d^* < 0$. That is to say, the parasite-positive equilibrium $E^* = (I_h^*, S_v^*, I_v^*)$ of system (2.3) is locally asymptotically stable if $d^* > 0$, unstable if $d^* < 0$.

Denote

$$\begin{pmatrix} f(I_h, I_v) \\ g(I_h, I_v) \end{pmatrix} = \begin{pmatrix} \beta_h I_v(N_h - I_h) - \mu_1 I_h \\ \beta_v I_h(S_v^0 - I_v) - \mu_2 I_v \end{pmatrix}.$$

Obviously, both f and $g : \mathbb{R}_+^2 \to \mathbb{R}$ are continuously differentiable maps. We have $\frac{\partial f}{\partial I_v} = \beta_h(N_h - I_h) - \mu_1 I_h \geq 0$, and $\frac{\partial g}{\partial I_h} = \beta_v(S_v^0 - I_v) - \mu_2 I_v \geq 0$. The system is cooperative in a domain $\mathbb{D} = \{(I_n, I_v) \in \mathbb{R}^2 : I_h \in [0, N_h], I_v \in [0, S_v^0]\}$. System (3.12) has a parasite-free equilibrium $(0,0)$ and a unique parasite-positive equilibrium E_1. According to Theorem 3.2.2 in [45], E_1 is globally attractive. Thus, the parasite-positive equilibrium E^* of sub-system (3.12) is globally asymptotically stable. This shows that the pathogenic effect may cause the system to be unstable and be responsible for the occurrence of sustained oscillations.

4. Bifurcation analysis

In this section, we will analyze the existence of forward bifurcation and Hopf bifurcation of system (2.3).

Theorem 4.1 System (2.3) exhibits a forward bifurcation from $E_S(0, \frac{K(r-\mu_2)}{r}, 0)$ when $R_0 = 1$. Furthermore, no backward bifurcation occurs.

Proof. The Jacobian matrix of system (2.3) at $E_S(0, \frac{K(r-\mu_2)}{r}, 0)$ is

$$J(E_S) = \begin{pmatrix} -\mu_1 & 0 & N_h\beta_h \\ -S_v^0\beta_v & \mu_2 - r & (1+\theta)\mu_2 - r \\ S_v^0\beta_v & 0 & -d - \mu_2 \end{pmatrix}.$$

Its eigenvalues are

$$\lambda_1 = \mu_2 - r, \lambda_2 = \frac{-b_0 - \sqrt{\Delta_0}}{2}, \lambda_3 = \frac{-b_0 + \sqrt{\Delta_0}}{2},$$

where

$$b_0 = \mu_1 + \mu_2 + d, \Delta_0 = \frac{4a^2bcK(r-\mu_2)}{rN_h} + (d - \mu_1 + \mu_2)^2.$$

Because all parameter values are non-negative, we know that λ_1 is always negative.
If $R_0 = 1$, then

$$c^* \triangleq \frac{rN_h\mu_1(d+\mu_2)}{a^2bK(r-\mu_2)}.$$

Substituting $c = c^*$ into λ_2 and λ_3, we have $\lambda_2 < 0, \lambda_3 = 0$. Also, the parasite-free equilibrium E_S is locally stable when $c < c^*$, and unstable when $c > c^*$. Therefore, $c = c^*$ is a bifurcation value.

We obtain a right eigenvector u and a left eigenvector $\bar{v}$ associated with the zero eigenvalue, where

$$\begin{aligned} u =&(u_1, u_2, u_3)^T = (abI_h, \frac{\mu_1(\theta\mu_2 - r - d)}{r-\mu_2}I_h, \mu_1 I_h)^T, \\ \bar{v} =&(\bar{v}_1, \bar{v}_2, \bar{v}_3) = (d + \mu_2, 0, ab). \end{aligned}$$

By the orthogonal condition $< u, \bar{v} >= 1$, we get

$$I_h^* = \frac{1}{ab(d+\mu_1+\mu_2)}.$$

By the transformation

$$I_h = x_1, S_v = x_2, I_v = x_3,$$

and noticing that system (2.3) has the form $\frac{dx}{dt} = f$, where $x = (x_1, x_2, x_3)^T$ and $f = (f_1, f_2, f_3)^T$, we have

$$\begin{aligned} x_1'(t) &= \beta_h x_3(t)(N_h - x_1(t)) - \mu_1 x_1(t) := f_1, \\ x_2'(t) &= r(x_2(t) + \theta x_3(t))(1 - \frac{x_2(t) + x_3(t)}{K}) - \beta_v x_2(t)x_1(t) - \mu_2 x_2(t) := f_2, \\ x_3'(t) &= \beta_v x_2(t)x_1(t) - dx_3(t) - \mu_2 x_3(t) := f_3. \end{aligned} \tag{4.1}$$

The formula of the bifurcation coefficient in system (4.1) at E_S is:

$$\bar{a} = \sum_{i,j,k=1}^{3} \bar{v}_i u_j u_k \frac{\partial^2 f_i}{\partial x_j \partial x_k}(E_S, c^*), \bar{b} = \sum_{i,j=1}^{3} \bar{v}_i u_j \frac{\partial^2 f_i}{\partial x_j \partial c}(E_S, c^*).$$

Since $\bar{v}_2 = 0$, what we need to consider are the cross derivatives of f_1 and f_3 in system (4.1) at the equilibrium E_S. We obtain some non-zero terms

$$\frac{\partial^2 f_1}{\partial x_1 \partial x_3} = \frac{\partial^2 f_1}{\partial x_3 \partial x_1} = -\beta_h,$$

$$\frac{\partial^2 f_3}{\partial x_1 \partial x_2} = \frac{\partial^2 f_3}{\partial x_2 \partial x_1} = \beta_v,$$

$$\frac{\partial^2 f_3}{\partial x_1 \partial c} = \frac{\partial^2 f_3}{\partial c \partial x_1} = \frac{a S_v^0}{N_h}.$$

Now we calculate the values of $\bar{a}$ and $\bar{b}$.

$$\begin{aligned}
\bar{a} =& \sum_{i,j,k=1}^{3} \bar{v}_i u_j u_k \frac{\partial^2 f_i}{\partial x_j \partial x_k}(E_S, c^*) \\
=& \bar{v}_1 \sum_{j,k=1}^{3} u_j u_k \frac{\partial^2 f_1}{\partial x_j \partial x_k}(E_S, c^*) + \bar{v}_3 \sum_{j,k=1}^{3} u_j u_k \frac{\partial^2 f_3}{\partial x_j \partial x_k}(E_S, c^*) \\
=& -\frac{2ab\mu_1(d+\mu_2)(abK(r-\mu_2)^2 + rN_h\mu_1(d+r-\theta\mu_2))}{N_h K (r-\mu_2)^2} I_h^{*2} < 0, \\
\bar{b} =& \sum_{i,j=1}^{3} \bar{v}_i u_j \frac{\partial^2 f_i}{\partial x_j \partial c}(E_S, c^*) \\
=& \bar{v}_3 u_1 \frac{\partial^2 f_3}{\partial x_1 \partial c}(E_S, c^*) \\
=& \frac{a^3 b^2 K(r-\mu_2)}{rN_h} I_h^* > 0.
\end{aligned}$$

From [41], we know that the local dynamical behavior of system (4.1) at equilibrium E_S is determined by the signs of $\bar{a}$ and $\bar{b}$. From the above calculation, we have $\bar{a} < 0$ and $\bar{b} > 0$. Thus, there exists a locally asymptotically stable endemic equilibrium of system (4.1) showing a forward bifurcation near the equilibrium E_S.

Remark 4.2 We conclude that no backward bifurcation occurs for system (4.1). The forward bifurcation of system (4.1) is shown by Figure 7 in Section 5.

For any parasite-positive equilibria $E^* = (I_h^*, S_v^*, I_v^*)$, the Jacobian matrix of system (2.3) at E^* is

$$J(E^*) = \begin{pmatrix} -I_v^*\beta_h - \mu_1 & 0 & (N_h - I_h^*)\beta_h \\ -S_v^*\beta_v & J_{22}^* & J_{23}^* \\ S_v^*\beta_v & I_h^*\beta_v & -d-\mu_2 \end{pmatrix},$$

where

$$J_{22}^* = r(1 - \frac{I_v^* + S_v^*}{K}) - I_h^*\beta_v - \mu_2 - \frac{r(S_v^* + \theta I_v^*)}{K}, J_{23}^* = r\theta(1 - \frac{I_v^* + S_v^*}{K}) - \frac{r(S_v^* + \theta I_v^*)}{K}. \quad (4.2)$$

The corresponding characteristic polynomial is

$$P(\xi; I_h^*, S_v^*, I_v^*) = \xi^3 + a_1\xi^2 + b_1\xi + c_1, \quad (4.3)$$

where

$$\begin{aligned}
a_1 =& d - J_{22}^* + I_v^*\beta_h + \mu_1 + \mu_2, \\
b_1 =& -J_{22}^*[d + I_v^*\beta_h + (\mu_1 + \mu_2)] + dI_v^*\beta_h - J_{23}^* I_h^*\beta_v + (I_h^* - N_h)S_v^*\beta_h\beta_v + d\mu_1 \\
&+ I_v^*\beta_h\mu_2 + \mu_1\mu_2, \\
c_1 =& -J_{22}^*[d\mu_1 + I_v^*\beta_h\mu_2 + \mu_1\mu_2 + dI_v^*\beta_h + I_h^* S_v^*\beta_h\beta_v - N_h S_v^*\beta_h\beta_v] + I_h^* N_h S_v^*\beta_h\beta_v^2 \\
&- J_{23}^*[I_h^*\beta_v\mu_1 + I_h^* I_v^*\beta_h\beta_v] - I_h^{*2} S_v^*\beta_h\beta_v^2,
\end{aligned}$$

J_{22}^*, J_{23}^* are defined by (4.2), S_v^* and I_v^* are defined in (3.2) and the coordinate of I_h^* is a positive root of (3.3).

From the above calculation and reference [46], we have the following theorem.

Theorem 4.3 The parasite-positive equilibrium E^* of system (2.3) undergoes
1) a static bifurcation if $c_1|_{E^*} = 0$ and $\Delta_{1,2}|_{E^*} > 0$;
2) a Hopf bifurcation if $\Delta_2 = 0, \frac{d\Delta_2}{d(Bif.)} \neq 0, \Delta_1|_{E^*} > 0$ and $c_1|_{E^*} > 0$.
Here a_1, b_1, c_1 are the coefficients of the characteristic polynomial (4.3), $d(Bif.)$ is the differentiation of the bifurcation parameter, and $\Delta_1 = a_1, \Delta_2 = a_1b_1 - c_1$ are the first and the second Hurwitz arguments, respectively.

5. Numerical results

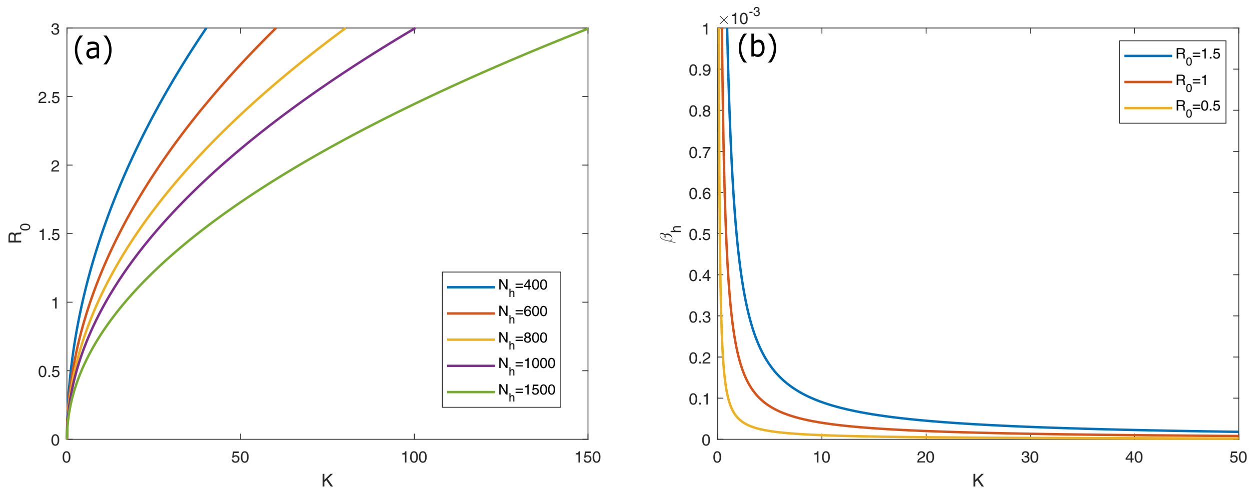

Figure 2. (a) The basic reproduction number R_0 as a function of the number of competent hosts (N_h) and the carrying capacity of bugs (K). (b) The impact of the transmission rate from infected bugs to susceptible competent hosts (β_h) and the carrying capacity of bugs (K) on the basic reproduction number R_0. The other parameter values are fixed as in (5.1).

In this section, we conduct numerical simulations for system (2.3) by using Matlab and Auto07P [47]. We choose the following parameter values,

$$\begin{aligned} &a = 0.6, b = 0.06, c = 0.49, r = 0.0274, \theta = 0.9, K = 1000, N_h = 400, \\ &\mu_1 = 0.0025, \mu_2 = 0.0083, d = 0.0246, \end{aligned} \tag{5.1}$$

which were also used in the reference [10]. It is easy to calculate that there are one vector-free equilibrium, one parasite-free equilibrium, and one parasite-positive equilibrium point with the above parameter values.

We study the effect of the number of competent hosts N_h and the carrying capacity of triatomine bugs K on the basic reproduction number of *T. rangeli* R_0. R_0 is proportional to K. Thus, R_0 increases as K increases. In particular, R_0 increases with an increasing number of hosts and the carrying capacity of bugs K. This is shown in Figure 2(a). R_0 depends on β_h, which is an important parameter and its expression is a combination of N_h and K. We find that the slopes of the curves increase when the number of competent hosts decreases. Because R_0 is related to β_h and K, the transmission rate from infected bugs to susceptible hosts is inversely proportional to the number of hosts, as shown in Figure 2(b). Figure 3(a) shows the occurrence of sustained oscillation as the parameter values are defined in (5.1) while Figure 3(b) illustrates the stability of the parasite-positive equilibrium in Theorem 3.4.

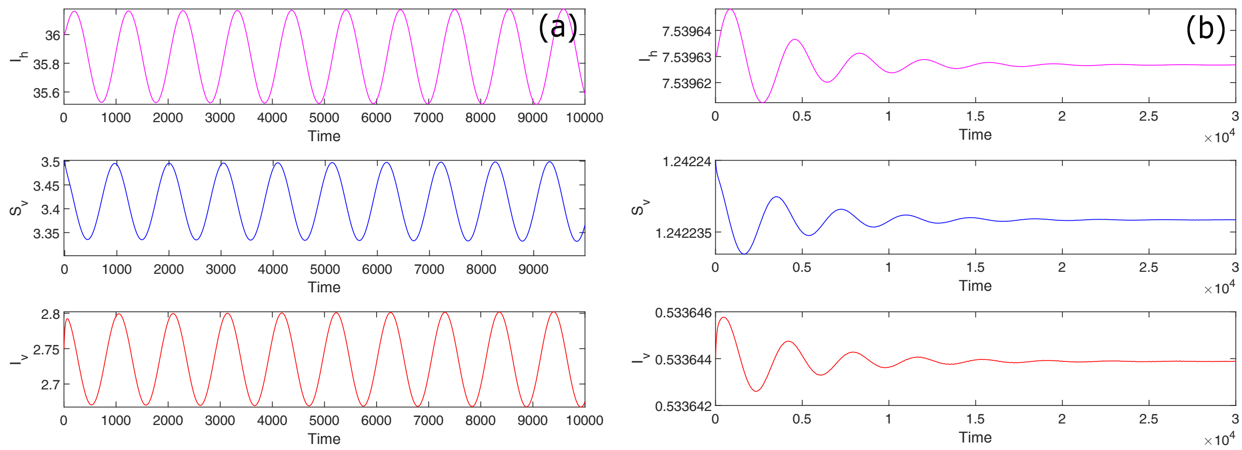

Figure 3. (a) A numerical solution of system (2.3) converges to a stable limit cycle. Parameter values are given in (5.1). The initial solution is $(I_h, S_v, I_v) = (36, 3.5, 2.75)$. Time series of $I_h(t), S_v(t), I_v(t)$, which is corresponding to the limit cycle in Figure 1; (b) A numerical solution of system (2.3) converging to a stable equilibrium. Parameter values are given in (5.1) except $r = 0.01$. The initial solution is $(I_h, S_v, I_v) = (7.53963, 1.24224, 0.533644)$.

Next, we consider the influence of the maximal number of offsprings that a triatomine bug produces per unit time (r), the carrying capacity of bugs (K), the pathogenic effect (d), and the transmission probability from infected hosts to susceptible triatomine bug per bite (c) in model (2.3) by using one-parameter and two-parameter bifurcation analysis.

We start with the maximal number of offsprings that a triatomine bug can produce per unit time. We choose r as the primary bifurcation parameter and keep the other parameters fixed as in (5.1). The one-parameter bifurcation diagram is shown in Figure 4. There exist two transcritical bifurcation points $TC_1(0, 0, 0)$ and $TC_2(0, 3.10847, 0)$ when $r = 8.3 \times 10^{-3}$ and $r = 8.326 \times 10^{-3}$, one supercritical Hopf bifurcation point $HB_1(1.94275, 3.12364, 0.135572)$ when $r = 9.39283 \times 10^{-3}$, and one supercritical Hopf bifurcation point $HB_2(8.18863, 3.17343, 0.580539)$ when $r = 1.23408 \times 10^{-2}$. The numbers of infected competent hosts, susceptible triatomine bugs and infected triatomine bugs will increase gradually when $0 < r < 9.39283 \times 10^{-3}$ and $r > 1.23408 \times 10^{-2}$. There is an unstable interval in which supercritical Hopf bifurcation occurs when $9.39283 \times 10^{-3} \leq r \leq 1.23408 \times 10^{-2}$. The red solid curve represents the stable limit cycle branch bifurcating from the supercritical Hopf bifurcation point, which indicates the appearance and the disappearance of stable limit cycle with the increase of the parameter r. Thus, when the maximal number of offsprings of susceptible triatomine bugs increases, the number of infected competent hosts and the number of infected triatomine bugs will increase out

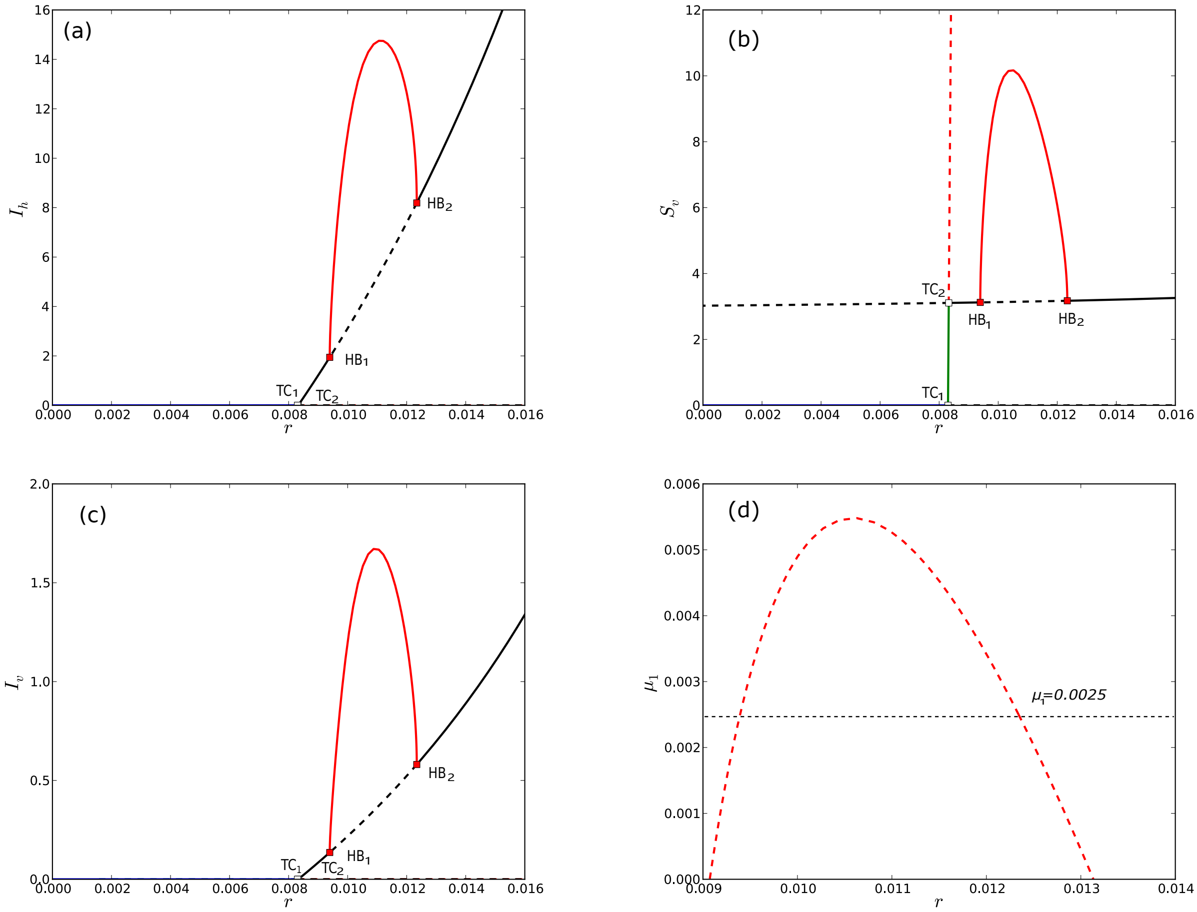

Figure 4. (a) One-parameter bifurcation diagram of system (2.3) showing the impact of r on I_h; (b) One-parameter bifurcation diagram of system (2.3) showing S_v vs. r; (c) One-parameter bifurcation diagram of system (2.3) showing I_v vs. r; (d) Two-parameter Hopf bifurcation diagram for system (2.3) showing r vs. μ_1. The dotted blue line is $\mu_1 = 0.0025$.

of the Hopf bifurcation interval $r \in [9.39283 \times 10^{-3}, 1.23408 \times 10^{-2}]$. Further, if we use μ_1 and r as the primary bifurcation parameters, then we obtain a two-parameter Hopf bifurcation curve, where the line $\mu_1 = 0.0025$ corresponds to the parameter values for Hopf bifurcation shown in Figure 4(a)–(c). The limit cycle branch connects the two Hopf bifurcation points and the period of limit cycle is finite. From Figure 4(d), we find that there are one or two Hopf bifurcation points when $0 \le \mu_1 \le 0.0055$, and no Hopf bifurcation occurs when $\mu_1 > 0.0055$.

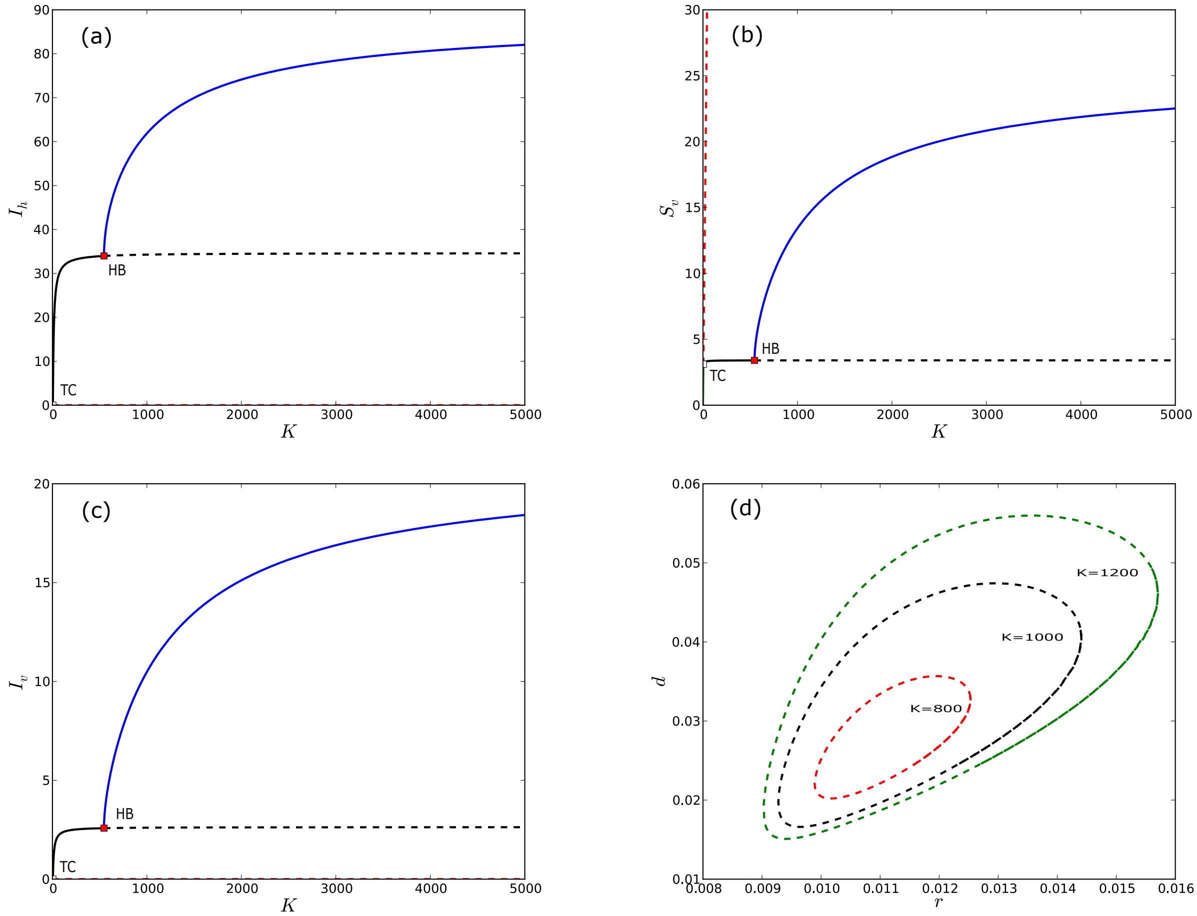

Figure 5. (a) One-parameter bifurcation diagram of system (2.3) showing K vs. I_h; (b) One-parameter bifurcation diagram of system (2.3) showing K vs. S_v; (c) One-parameter bifurcation diagram of system (2.3) showing K vs. I_v; (d) Two-parameter Hopf bifurcation diagram for system (2.3) showing r vs. d when $K = 800, 1000, 1200$, respectively.

The carrying capacity of triatomine bugs is the number that the ecosystem can sustainably support. It may vary due to many factors. We also use the carrying capacity K as the primary bifurcation parameter. With $\theta = 0.3$, we obtain the one-parameter bifurcation diagram for system (2.3) shown in Figure 5. There are one transcritical bifurcation point $TC(0, 3.10847, 0)$ and one supercritical Hopf bifurcation point $HB(33.9734, 3.39698, 2.57824)$ when $K = 4.45926$ and $K = 5.45626 \times 10^2$, respectively. The amplitudes and periods of limit cycles bifurcating from HB become larger as K increases. When the carrying capacity of susceptible triatomine bugs increases, there will be always a supercritical Hopf bifurcation point, i.e., all the state variables will vary periodically, and all the competent hosts, susceptible triatomine bugs and infected triatomine bugs will coexist. In addition, if we use r and d as the primary two bifurcation parameters, then we obtain the two-parameter Hopf bifurcation curves which are all closed curves when $K = 800, 1000, 1200$, respectively. This also indicates that no Bogdanov-Takens bifurcation of the parasite-positive equilibrium occurs for system (2.3).

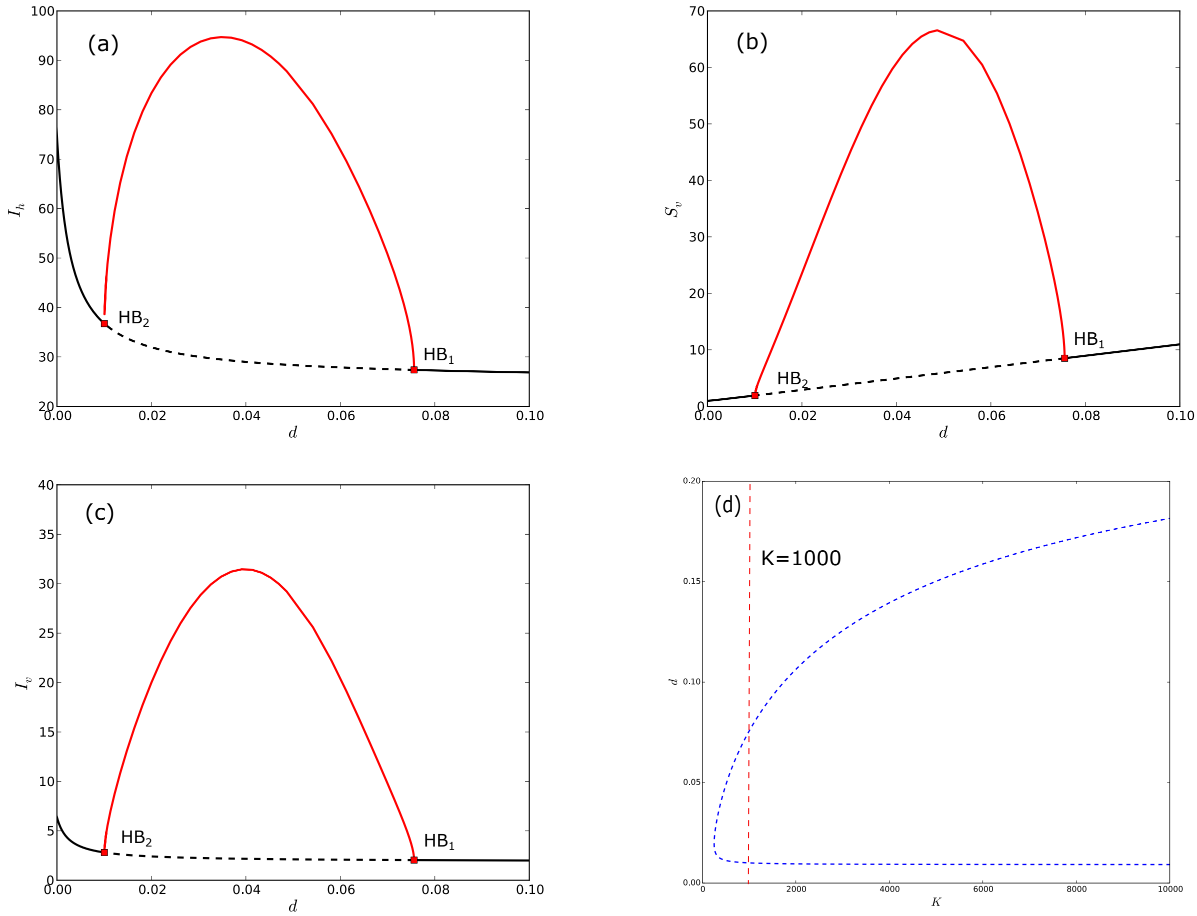

Figure 6. (a) One-parameter bifurcation diagram of system (2.3) showing d vs. I_h; (b) One-parameter bifurcation diagram of system (2.3) showing d vs. S_v; (c) One-parameter bifurcation diagram of system (2.3) showing d vs. I_v; (d) Two-parameter Hopf bifurcation diagram for system (2.3) showing d vs. K when $\theta = 0.2$.

Next, we use d as the primary bifurcation parameter to study the influence of the pathogenic effect in system (2.3). The parameter θ is set to 0.2 and other parameters are fixed as in (5.1). We obtain the one-parameter bifurcation diagram, shown in Figure 6(a)–(c). There are two supercritical Hopf bifurcation points $HB_1(27.3612, 8.51017, 2.03959)$ and $HB_2(36.7308, 1.90856, 2.80866)$ when $d = 0.0756105$ and $d = 0.0100453$, respectively. Thus, when the death rate of infected vectors increases due to the strong pathogenic effect, the number of the competent hosts and infected triatomine bugs will decrease, and the number of susceptible triatomine bugs will increase except an unstable interval for the occurrence of Hopf bifurcation. Two-parameter Hopf bifurcation curve is also given to illustrate the occurrence of

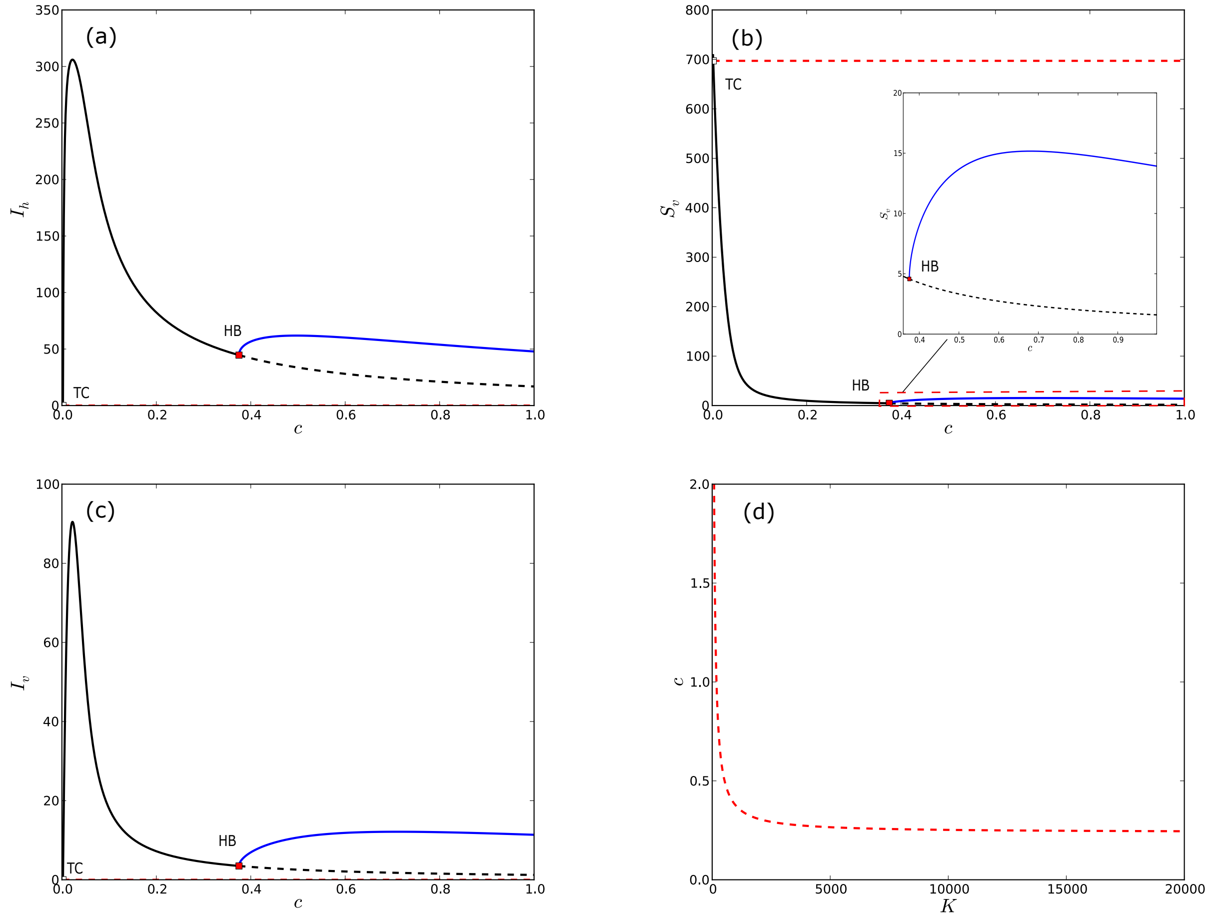

Figure 7. (a) One-parameter bifurcation diagram of system (2.3) showing c vs. I_h; (b) One-parameter bifurcation diagram of system (2.3) showing c vs. S_v; (c) One-parameter bifurcation diagram of system (2.3) showing c vs. I_v; (d) Two-parameter Hopf bifurcation diagram for system (2.3) showing c vs. K.

stable limit cycles (Figure 6(d)), where the red dotted line is $K = 1000$. Hopf bifurcation will always occur when $K \geq 252.498$.

The transmission rate from infected competent hosts to susceptible bugs (β_v) depends on the number of bites per triatomine bug per unit time (a) and the transmission probability from infected hosts to susceptible triatomine bugs per bite (c). Since the two parameters a and c have a similar role in β_v, for simplicity, we only use c as the primary bifurcation parameter and fix $\theta = 0.3$. We obtain the one-parameter bifurcation diagram (Figure 7(a)–(c)). There is a transcritical bifurcation point $TC(0, 6.9708 \times 10^2, 0)$ when $c = 2.18504 \times 10^{-2}$, which confirms the forward bifurcation as shown in Theorem 3.1. The numbers of infected hosts and infected vectors will increase firstly, then decrease dramatically to a low level. The appearance of the limit cycle indicates that *T. rangeli* parasites will persist with the increase of the transmission probability from infected hosts to susceptible triatomine bugs per bite. Also, there is a supercritical Hopf bifurcation point $HB(44.6167, 4.57113, 348737)$ when $c = 0.375043$. The amplitudes and periods of limit cycles bifurcating from HB become larger as c increases. From Figure 7, we can see that all state variables coexist once the number of bites of per triatomine bug per unit time is greater than 0.865432. Therefore, *T. rangeli* parasites will always persist if the infection rates of susceptible triatomine bug and infected triatomine bug increase. The two-parameter (c *vs.* K) Hopf bifurcation curve of system (2.3) is given in Figure 7(d), which tells the relationship of the carrying capacity and the transmission probability from infected hosts to susceptible triatomine bug per bite. There is only one supercritical Hopf bifurcation occurring for system (2.3).

From the above analysis, we know that the dynamics of triatomine bugs in system (2.3) are similar to HIV dynamics in [41, 48]. System (2.3) undergoes a forward bifurcation instead of a backward bifurcation. However, from the limit cycle branches in Figures 5(a)–(c) and 7(a)–(c), we conclude that the *T. rangeli* parasites relevant to Chagas disease will persist due to the sustained oscillations from Hopf bifurcation when the carrying capacity (K) or the transmission probability (c) increases. Thus, it is challenging to eliminate *T. rangeli* parasites, a sister trypanosoma to *T. cruzi* and commonly causing the misdiagnosis of the Chagas disease.

Comparing with the dynamics of model (2.3) and revisiting model (2.1) numerically, we find that model (2.1) with Ricker's type function in [10] also doesn't undergo Bagdanov-Takens bifurcation at the parasite-positive equilibrium. However, model (2.1) has periodic-doubling bifurcation of limit cycles for r, the maximal number of offsprings that a triatomine bug can produce per unit time. This indicates the occurrence of chaos for model (2.1), which differs from the dynamics of model (2.3).

6. Discussion and conclusions

In this paper, we have formulated a model with a logistic growth of of triatmine bugs to study the dynamics of infected competent hosts, susceptible and infected triatomine bugs. The existence and stability of the vector-free equilibrium, parasite-free equilibrium and the parasite-positive equilibrium are studied. The direction of transcritical bifurcation and Hopf bifurcation is also investigated. Numerical simulations are conducted to illustrate and expand the theoretical results.

For many infectious disease models, the disease-free equilibrium usually loses its stability when R_0 increases to cross one, which results in a bifurcation where a curve of endemic equilibria emerges. The direction of this bifurcation is forward if the endemic curve occurs when R_0 is slightly above 1 and there is no parasite-positive equilibrium near the disease-free equilibrium for $R_0 < 1$. In contrast, the bifurcation is backward if the bifurcating equilibrium occurs when $R_0 < 1$. Basically, a backward bifurcation implies the occurrence of multiple endemic equilibria and the coexistence of a stable endemic equilibrium with a stable disease-free equilibrium. Thus, a forward bifurcation indicates that the infectious disease may be cured while it is not easy to eliminate the disease when a backward bifurcation occurs. Model (2.3) only goes through the forward bifurcation. However, this doesn't mean that the disease would be eliminated. The persistence of sustained oscillations of *T. rangeli* makes the disease eradication challenging.

One-parameter bifurcation diagrams for the parameters r, K, d, c are showed, respectively. Oscillations always persists as K or c increases. This shows that the *Trypanosoma rangeli* will always exist in all the population and it is difficult to be eliminated. Bagdanov-Takens bifurcation of the parasite-positive equilibrium doesn't occur in models (2.1) and (2.3). Using numerical simulations, we also find that model (2.1) with Ricker's type function growth rather than the logistic function growth could go though periodic-doubling bifurcation of limit cycles when the maximal number of offsprings that a triatomine bug can produce per unit time (r) increases. This suggests the emergence of chaos for model (2.1).

The pathogenic effect to the triatomine bug population is also studied. This may provide some critical insights for the prevention and control of Chagas disease. Although *T. rangeli* is not pathogenic to human, it is pathogenic to triatomine bugs, which have a great effect on the dynamics of *T. cruzi* population and triatomine bug population. It can cause the model to lose stability and undergo Hopf bifurcation. Moreover, the amplitudes of oscillations become larger as the parameters K or c increases. It is worth noting that we illustrate the non-existence of Bagdanov-Takens bifurcation of the parasite-positive equilibrium numerically without providing analytical results due to too many parameters in model (2.3). This work provides more information that improves our understanding of the complexity of host-parasite-vector interactions.

Acknowledgments

The authors are very grateful to Professor Jianhong Wu for his helpful suggestions. This work was partially supported by the National Natural Science Foundation of China (No. 11671114) and NSF of Zhejiang (LY20A010002). X. Wu is supported by NSF of China (No.12071300). L. Rong is supported by the NSF grant DMS-1950254.

Conflict of interest

The authors declare there is no conflict of interest.

References

1. P. Bernard, B. Carolina, S. Eric, R. Isabella, V. Rafael, G. Joaquim, The benefit trial: Where do we go from here?, *PLoS Neg. Trop. Dis.*, **10** (2016), 1–4. https://doi.org/10.1371/journal.pntd.0004343

2. B. Y. Lee, S. M. Bartsch, L. Skrip, D. L. Hertenstein, A. Galvani, Are the london declaration's 2020 goals sufficient to control chagas disease?: Modeling scenarios for the yucatan peninsula, *PLoS Neg. Trop. Dis.*, **12** (2018), 1–20. https://doi.org/10.1371/journal.pntd.0006337

3. World Health Organization, Chagas disease in Latin America: an epidemiological update based on 2010 estimates, *Weekly Epidemiol. Record*, **90** (2015), 33–43.

4. C. H. Imperador, F. Madeira, M. T. Oliveira, A. B. Oliveira, K. C. Alevi, Parasite-vector interaction of chagas disease: A mini-review, *Amer. J. Trop. Med, Hyg.*, **98** (2018), 653–655. https://doi.org/10.4269/ajtmh.17-0657

5. A. R. Méndez, E. Aldasoro, E. D. Lazzari, E. Sicuri, M. Brown, D. A. J. Moore, et al., Prevalence of chagas disease in latin-american migrants living in Europe: A systematic review, meta-analysis, *PLoS Neg. Trop. Dis.*, **9** (2015), 1–15. https://doi.org/10.1371/journal.pntd.0003540

6. P. J. Plourde, K. Kadkhoda, M. Ndao, Congenitally transmitted chagas disease in canada: a family cluster, *Can. Medi. Asso. J.*, **189** (2017), 1489–1492. https://doi.org/10.1503/cmaj.170648

7. C. Hernández, Z. Cucunubá, E. Parra, G. Toro, P. Zambran, J. D. Ramírez, COVID-19: implications for people with Chagas disease, *Heart*, **15** (2020), 69. https://doi.org/10.5334/gh.891

8. E. J. Zaidel, Chagas disease (Trypanosoma cruzi) and HIV co-infection in Colombia, *Inter. J. Infect. Dis.*, **26** (2014), 146–148. https://doi.org/10.1016/j.ijid.2014.04.002

9. N. Tomasini, P. G. Ragone, S. Gourbire, J. P. Aparicio, P. Diosque, Epidemiological modeling of trypanosoma cruzi: Low stercorarian transmission and failure of host adaptive immunity explain the frequency of mixed infections in humans, *PLoS Comput. Biol.*, **13** (2017), 1–21. https://doi.org/10.1371/journal.pcbi.1005532

10. X. T. Wu, D. Z. Gao, Z. L. Song, J. H. Wu, Modelling triatomine bug population and trypanosoma rangeli transmission dynamics: co-feeding, pathogenic effect and linkage with chagas disease, *Math. Bios.*, **324** (2020), 1–14. https://doi.org/10.1016/j.mbs.2020.108326

11. S. S. Weber, S. Noack, P. M. Selzer, R. Kaminsky, Blocking transmission of vector borne diseases, *Inter. J. Paras.: Drugs Drug Resist.*, **7** (2017), 90–109. https://doi.org/10.1016/j.ijpddr.2017.01.004

12. N. Tomasini, P. G. Ragone, S. Gourbire, J. P. Aparicio, P. Diosque, Epidemiological modeling of trypanosoma cruzi: low stercorarian transmission and failure of host adaptive immunity explain the frequency of mixed infections in humans, *PLoS Comput. Biol.*, **13** (2017), 1–21. https://doi.org/10.1371/journal.pcbi.1005532

13. M. A. A. Zegarra, D. Olmos-Liceaga, J. X. Velasco-Hernández, The role of animal grazing in the spread of chagas disease, *J. Theor. Biol.*, **457** (2018), 19–28. https://doi.org/10.1016/j.jtbi.2018.08.025

14. R. C. Ferreira, C. F. Teixeira, V. F. A. de Sousa, A. A. Guarneri, Effect of temperature and vector nutrition on the development and multiplication of trypanosoma rangeli in rhodnius prolixus, *Parasitol. Res.*, **117** (2018), 1737–1744. https://doi.org/10.1007/s00436-018-5854-2

15. A. A. Guarneri, M. G. Lorenzo, Triatomine physiology in the context of trypanosome infection, *J. Insect. Physiol.*, **97** (2017), 66–76. https://doi.org/10.1016/j.jinsphys.2016.07.005

16. J. K. Peterson, S. M. Bartsch, B. Y. Lee, A. P. Dobson, Broad patterns in domestic vector-borne trypanosoma cruzi transmission dynamics: synanthropic animals and vector control, *Paras. & Vectors*, **8** (2015), 1–10. https://doi.org/10.1186/s13071-015-1146-1

17. J. K. Peterson, A. L. Graham, What is the true effect of Trypanosoma rangeli on its triatomine bug vector?, *J. Vector Ecol.*, **41** (2016), 27–33. https://doi.org/10.1111/jvec.12190

18. L. D. Ferreira, M. H. Pereira, A. A. Guarneri, Revisiting trypanosoma rangeli transmission involving susceptible and non-susceptible hosts, *PLoS One*, **10** (2015), 1–14. https://doi.org/10.1371/journal.pone.0140575

19. S. E. Randolph, L. Gern, P. A. Nuttall, Co-feeding ticks: Epidemiological significance for tick-borne pathogen transmission, *Parasitol. Today*, **12** (1996), 472–479. https://doi.org/10.1016/S0169-4758(96)10072-7

20. M. J. Voordouw, Co-feeding transmission in Lyme disease pathogens, *Parasitology*, **142** (2015), 290–302. https://doi.org/10.1017/S0031182014001486

21. K. Nah, F. M. Magpantay, Á. Bede-Fazekas, G. Röst, J. H. Wu, Assessing systemic and non-systemic transmission risk of tick-borne encephalitis virus in Hungary, *PLoS One*, **14** (2019), 1–18. https://doi.org/10.1371/journal.pone.0217206

22. X. Zhang, X. T. Wu, J. H. Wu, Critical contact rate for vector-host-pathogen oscillation involving co-feeding and diapause, *J. Biol. Syst.*, **25** (2017), 1–19. https://doi.org/10.1142/S0218339017400083

23. J. X. Velasco-Hernández, An epidemiological model for the dynamics of chagas disease, *Biosystems*, **26** (1991), 127–134. https://doi.org/10.1016/0303-2647(91)90043-K

24. J. X. Velasco-Hernández, A model for chagas disease involving transmission by vectors and blood transfusion, *Theor. Pop. Biol.*, **46** (1994), 1–31. https://doi.org/10.1006/tpbi.1994.1017

25. M. A. Acuña-Zegarra, D. O. Liceaga, J. X. Velasco-Hernández, The role of animal grazing in the spread of chagas disease, *J. Theor. Biol.*, **457** (2018), 19–28. https://doi.org/10.1016/j.jtbi.2018.08.025

26. C. M. Kribs, C. Mitchell, Host switching vs. host sharing in overlapping sylvatic trypanosoma cruzi transmission cycles, *J. Biol. Dyn.*, **9** (2015), 1–31. https://doi.org/10.1080/17513758.2015.1075611

27. G. E. Ricardo, C. A. Leonardo, K. O. Paula, A. L. Leonardo, S. Raúl, K. Uriel, Strong host-feeding preferences of the vector triatoma infestans modified by vector density: Implications for the epidemiology of chagas disease, *PLoS Neg. Trop. Dis.*, **3** (2009), 1–12. https://doi.org/10.1371/journal.pntd.0000447

28. L. Stevens, D. M. Rizzo, D. E. Lucero, J. C. Pizarro, Household model of chagas disease vectors (hemiptera: Reduviidae) considering domestic, peridomestic, and sylvatic vector populations, *J. Med. Entomol.*, **50** (2013), 907–915. https://doi. org/10.1603/ME12096

29. C. J. Schofield, N. G. Williams, T. F. D. C. Marshall, Density-dependent perception of triatomine bug bites, *Ann. Trop. Med. Paras.*, **80** (1986), 351–358. https://doi.org/10.1080/00034983.1986.11812028

30. R. Gurgel-Goncalves, C. Galvão, J. Costa, A. T. Peterson, Geographic distribution of chagas disease vectors in brazil based on ecological niche modeling, *J. Trop. Med.*, **2012** (2012), 1–15. https://doi.org/10.1155/2012/705326

31. L. Frédéric, Niche invasion, competition and coexistence amongst wild and domestic bolivian populations of chagas vector triatoma infestans (hemiptera, reduviidae, triatominae), *Comptes Rendus Biol.*, **336** (2013), 183–193. https://doi.org/10.1016/j.crvi.2013.05.003

32. C. M. Barbu, A. Hong, J. M. Manne, D. S. Small, E. J. Q. Caldern, K. Sethuraman, et al., The effects of city streets on an urban disease vector, *PLoS Comput. Biol.*, **9** (2013), 1–9. https://doi.org/10.1371/journal.pcbi.1002801

33. H. Inaba, H. Sekine, A mathematical model for chagas disease with infection-age-dependent infectivity, *Math. Biosci.*, **190** (2004), 39–69. https://doi.org/10.1016/j.mbs.2004.02.004

34. C. Barbu, E. Dumonteil, S. Gourbière, Optimization of control strategies for non-domiciliated triatoma dimidiata, chagas disease vector in the yucatan peninsula, Meaxico, *PLoS Neg. Trop. Dis.*, **3** (2009), 1–10. https://doi.org/10.1371/journal.pntd.0000416

35. M. Z. Levy, F. S. M. Chavez, J. G. Cornejo, C. del Carpio, D. A. Vilhena, F. E. Mckenzie, et al., Rational spatio-temporal strategies for controlling a chagas disease vector in urban environments, *J. R. Soc. Interface*, **7** (2010), 1061–1070. https://doi.org/10.1098/rsif.2009.0479

36. R. E. Guëtler, U. Kitron, M. C. Cecere, E. L. Segura, J. E. Cohen, Sustainable vector control and management of chagas disease in the gran chaco, Argentina, *Proc. Nat. Acad. Sci. U. S. A.*, **104** (2007), 16194–16199. https://doi.org/10.1073/pnas.0700863104

37. B. Y. Lee, K. M. Bacon, A. R. Wateska, M. E. Bottazzi, E. Dumonteil, P. J. Hotez, Modeling the economic value of a chagas' disease therapeutic vaccine, *Hum. Vaccines & Immunother.*, **8** (2012), 1293–1301. https://doi.org/10.4161/hv.20966

38. B. Y. Lee, K. M. Bacon, M. E. Bottazzi, P. J. Hotez, Global economic burden of chagas disease: a computational simulation model, *Lancet Infect. Dis.*, **13** (2013), 342–348. https://doi.org/10.1016/S1473-3099(13)70002-1

39. J. E. Rabinovich, J. A. Leal, D. F. de Pinero, Domiciliary biting frequency and blood ingestion of the chagasis disease vector rhodnius prolixus stahl (hemiptera: reduviidae in Venezuela), *Trans. R. Soc. Trop. Med. Hyg.*, **73** (1979), 272–283. https://doi.org/10.1016/0035-9203(79)90082-8

40. P. Driessche, J. Watmough, Reproduction numbers and sub-threshold endemic equilibria for compartmental models of disease transmission, *Math. Bios.*, **180** (2002), 29–48. https://doi.org/10.1016/S0025-5564(02)00108-6

41. Y. C. Xu, Z. R. Zhu, Y. Yang, F. W. Meng, Vectored immunoprophylaxis and cell-to-cell transmission in HIV dynamics, *Inter. J. Bifur. Chaos*, (2020), 1–19. https://doi.org/10.1142/S0218127420501850

42. M. Y. Li, S. M. James, A geometric approach to global-stability problems, *SIAM J. Math. Anal.*, **27** (1996), 1070–1083. https://doi.org/10.1137/S0036141094266449

43. M. Y. Li, J. R. Graef, L. Wang, J. Karsai, Global dynamics of a seir model with varying total population size, *Math. Bios.*, **160** (1999), 191–213. https://doi.org/10.1016/S0025-5564(99)00030-9

44. R. H. Martin, Logarithmic norms and projections applied to linear differential systems, *J. Math. Anal. Appl.*, **45** (1974), 432–454. https://doi.org/10.1016/0022-247X(74)90084-5

45. H. L. Smith, Monotone dynamical systems: an introduction to the theory of competitive and cooperative systems, *Am. Math. Soc. Math. Surv. Monogr.*, 1995. https://doi.org/http://dx.doi.org/10.1090/surv/041

46. W. J. Zhang, R. Bhagavath, N. Madras, J. Heffernan, Examining HIV progression mechanisms via mathematical approaches, *Math. Appl. Sci. Eng.*, **99** (2020), 1–24. https://doi.org/10.5206/mase/10774

47. E. J. Doedel, B. E. Oldeman, *AUTO-07P:Continuation and bifurcation software for ordinary differential equations*, Technical report, Concordia University, 2009. https://doi.org/US5251102A

48. Y. C. Xu, Y. Yang, F. W. Meng, P. Yu, Modeling and analysis of recurrent autoimmune disease, *Nonl. Anal.: Real World Appl.*, **54** (2020), 1–28. https://doi.org/10.1016/j.nonrwa.2020.103109